

Supporting Information for

Simultaneously achieving ultrahigh energy storage density and high efficiency in BiFeO₃-based relaxor ferroelectric ceramics via highly disordered multicomponent design

Tao Cui¹, Ji Zhang^{1,*}, Jian Guo², Xiongjie Li³, Shun Guo¹, Yu Huan⁴, Jing Wang^{5,*}, Shan-Tao Zhang²

¹ School of Materials Science and Engineering, Nanjing University of Science and Technology, Nanjing, 210094, China

² National Laboratory of Solid State Microstructures, Department of Materials Science and Engineering, College of Engineering and Applied Science & Jiangsu Key Laboratory of Artificial Functional Materials & Collaborative Innovation Center of Advanced Microstructures, Nanjing University, Nanjing 210093, China

³ Wuhan National Laboratory for Optoelectronics, Huazhong University of Science and Technology, Wuhan, Hubei 430074, China

⁴ School of Material Science and Engineering, University of Jinan, Jinan, 250022, China

⁵ State Key Laboratory of Mechanics and Control of Mechanical Structures, College of Aerospace Engineering, Nanjing University of Aeronautics and Astronautics, Nanjing 210016, China

*Corresponding authors: jizhang@njust.edu.cn; wang-jing@nuaa.edu.cn

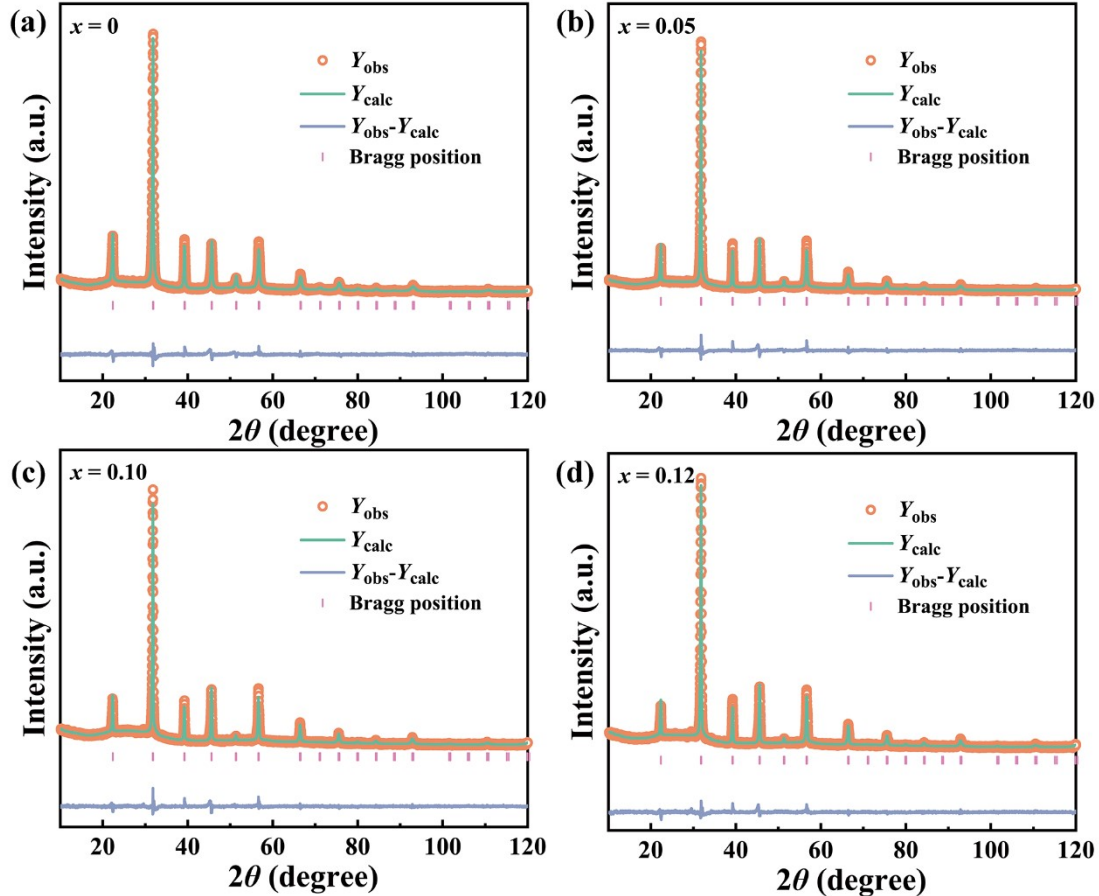


Fig. S1 Refined XRD patterns of (a) $x = 0$, (b) $x = 0.05$, (c) $x = 0.10$, (d) $x = 0.12$

Table S1 Refined structural parameters of BLF-BST-KNN ceramics.

	$x = 0$	$x = 0.05$	$x = 0.08$	$x = 0.10$	$x = 0.12$
Space group	$Pm-3m$	$Pm-3m$	$Pm-3m$	$Pm-3m$	$Pm-3m$
$a=b=c$	3.97461 Å	3.97875 Å	3.97892 Å	3.97951 Å	3.97948 Å
$\alpha=\beta=\gamma$	90°	90°	90°	90°	90°
Cell volume	62.789	62.986	62.993	63.022	63.020
R_{wp}	3.80	3.89	3.44	3.51	3.72
R_p	2.71	2.69	2.48	2.53	2.66
χ^2	3.64	3.54	2.50	2.52	2.92

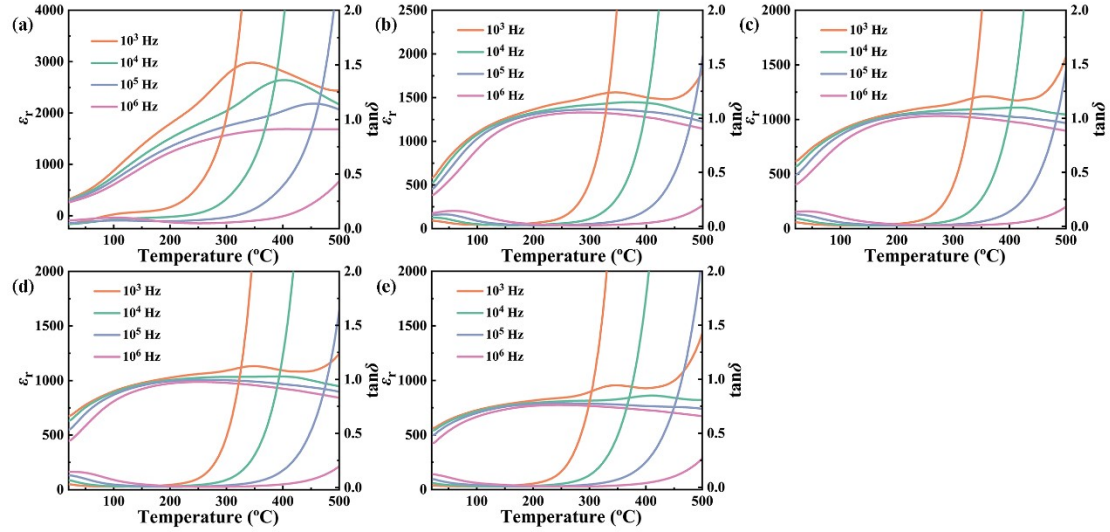


Fig. S2 Temperature-dependent ϵ_r and $\tan\delta$ at various frequencies: (a) $x = 0$, (b) $x = 0.05$, (c) $x = 0.08$, (d) $x = 0.10$, (e) $x = 0.12$.

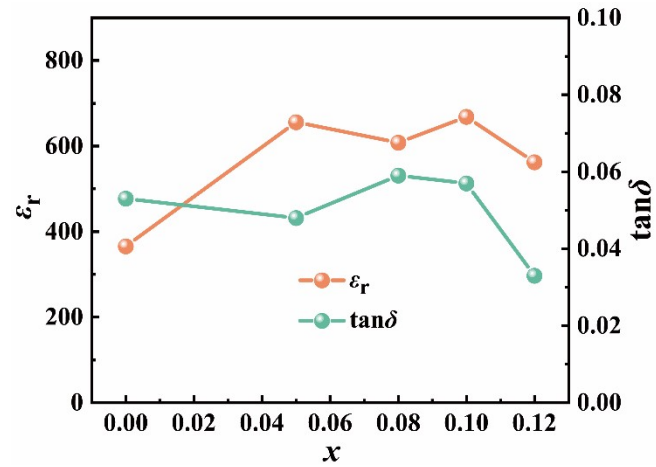


Fig. S3 Composition dependent room temperature ϵ_r and $\tan\delta$ values measured at 10 kHz.

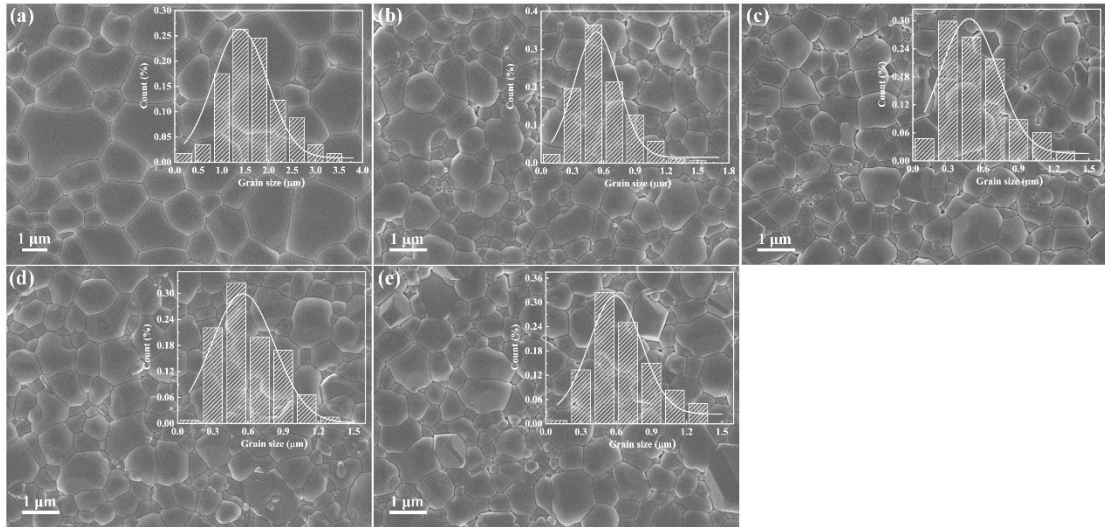


Fig. S4 Typical SEM morphologies of BLF-BST-KNN ceramics: (a) $x = 0$, (b) $x = 0.05$, (c) $x = 0.08$, (d) $x = 0.10$, (e) $x = 0.12$. The corresponding insets show the grain size distribution.

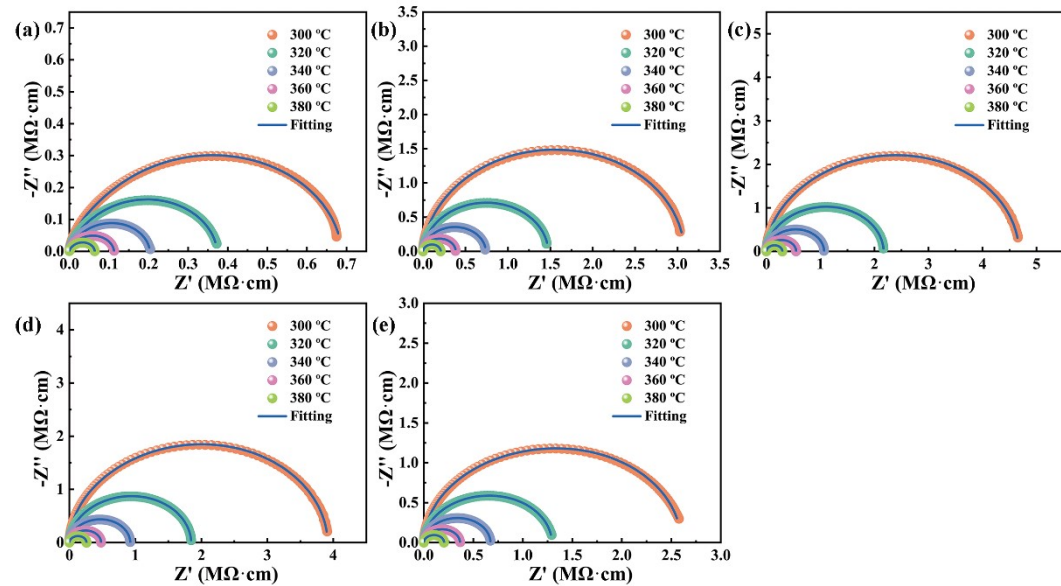


Fig. S5 Impedance spectra of BLF-BST-KNN ceramics at different temperature: : (a) $x = 0$, (b) $x = 0.05$, (c) $x = 0.08$, (d) $x = 0.10$, (e) $x = 0.12$.

Table S2 Total resistivity of BLF-BST-KNN ceramics extracted from corresponding impedance spectra.

	$x = 0$	$x = 0.05$	$x = 0.08$	$x = 0.10$	$x = 0.12$
300°C	0.68813	3.11292	4.3131	4.04033	2.65651
320°C	0.37336	1.4922	1.98776	1.90616	1.32055
340°C	0.20351	0.74817	0.97265	0.95274	0.68785
360°C	0.1129	0.39073	0.49	0.49672	0.37336
380°C	0.06413	0.21143	0.25507	0.26806	0.20923

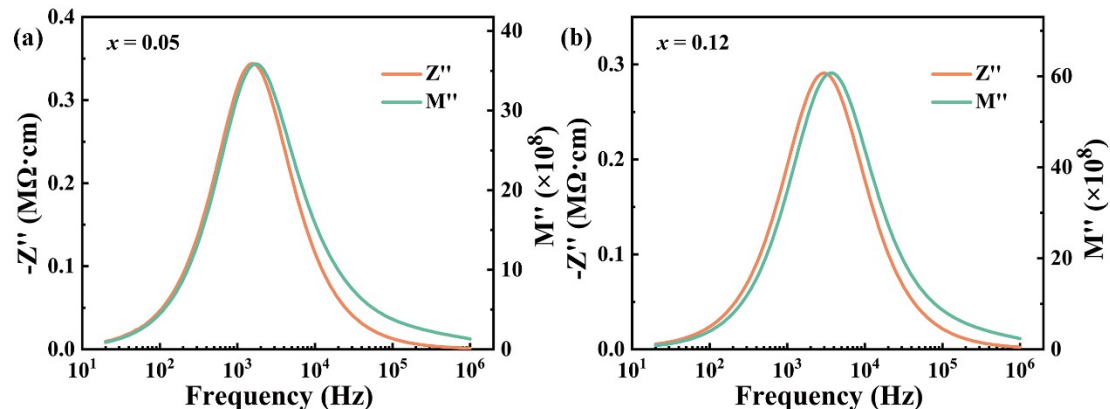


Fig. S6 Combined patterns of Z'' and M'' under various frequencies at 340°C: (a) $x = 0.05$, (b) $x = 0.12$.

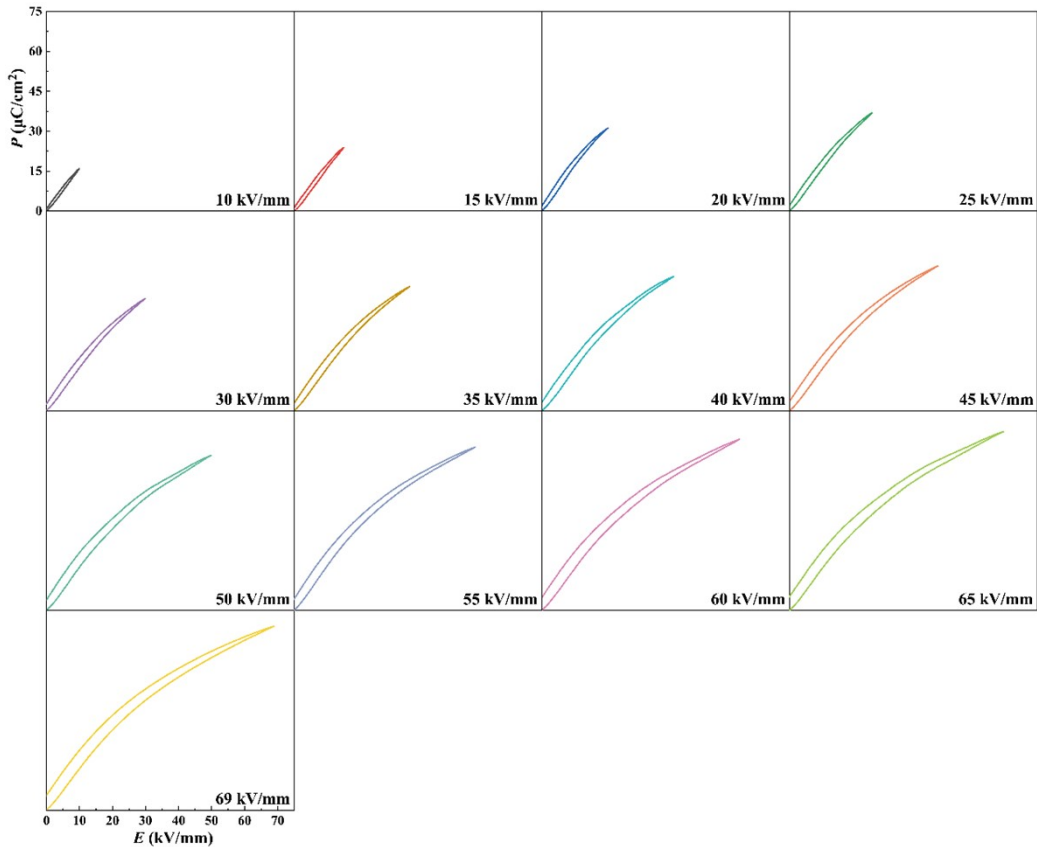


Fig. S7 Room temperature unipolar P - E curves of $x = 0.08$ at various electric fields.

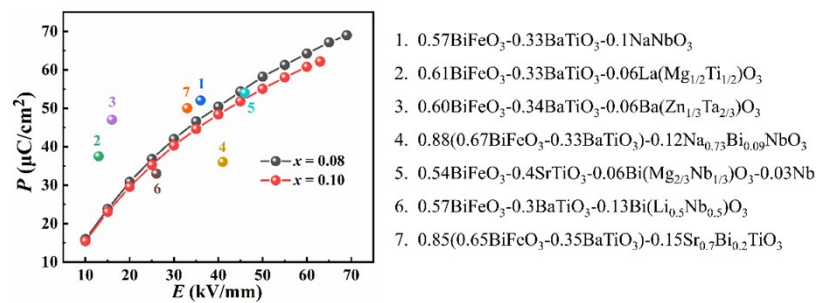


Fig. S8 The comparison of P_{\max} values between this work and other reports.

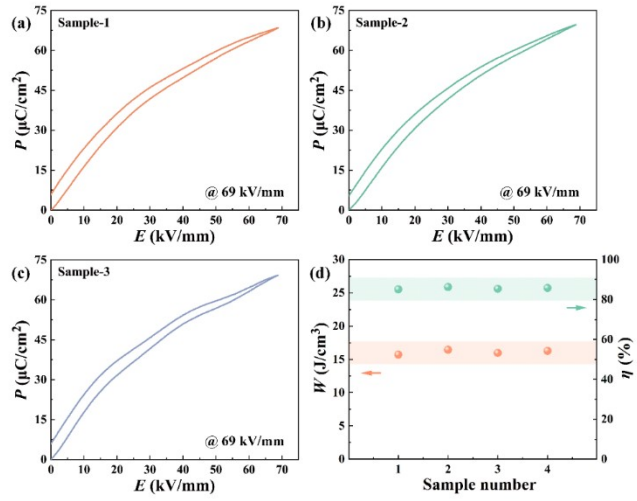


Fig. S9 (a-c) P - E curves of samples 1-3 for $x = 0.08$, respectively. (d) W_{rec} and η of the four samples (including the one shown in Fig. 4).

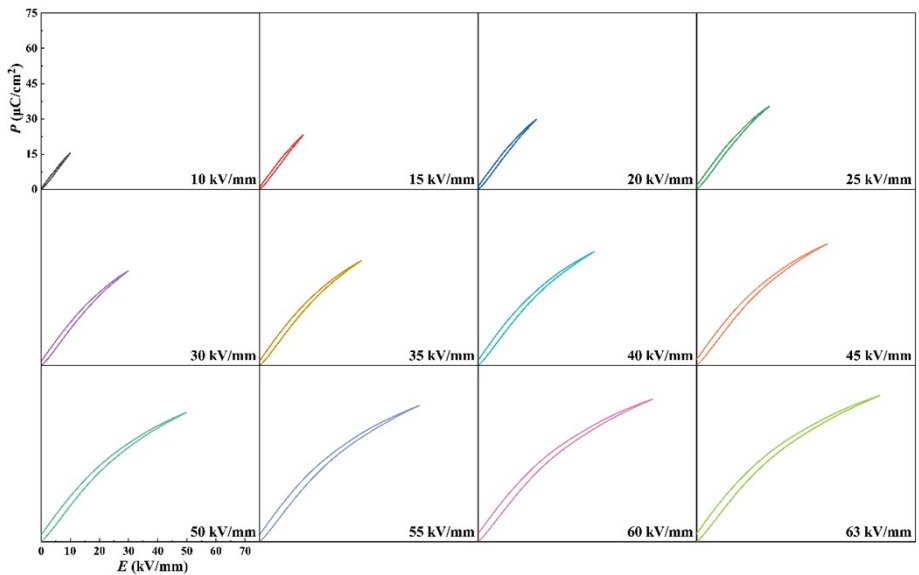


Fig. S10 Room temperature unipolar P - E curves of $x = 0.10$ at various electric fields.

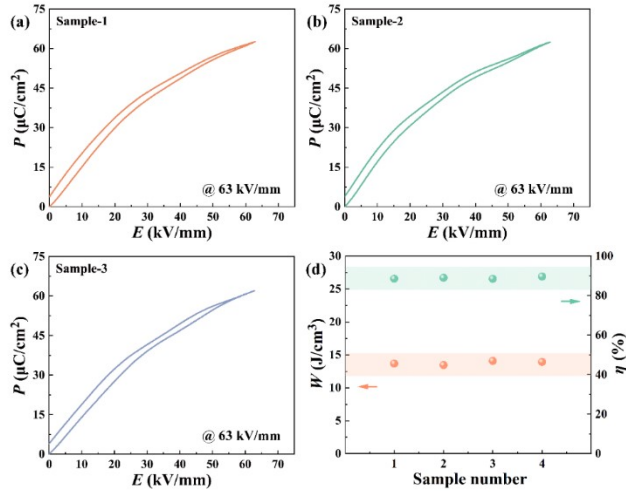


Fig. S11 (a-c) P - E curves of samples 1-3 for $x = 0.10$, respectively. (d) W_{rec} and η of the four samples (including the one shown in Fig. 4).

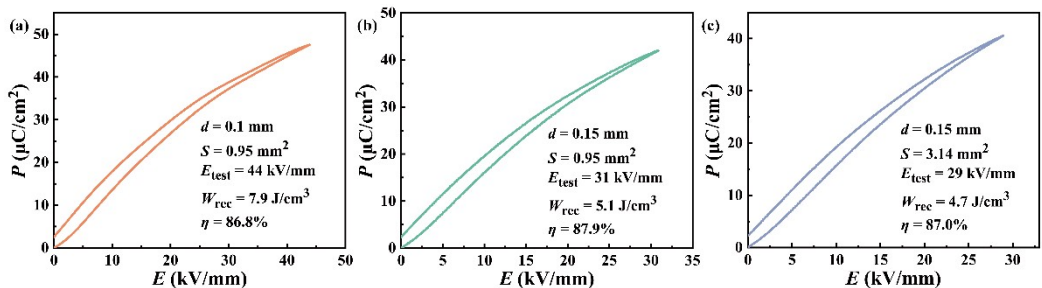


Fig. S12 P - E curves of $x = 0.08$ ceramic with different thickness and electrode area.

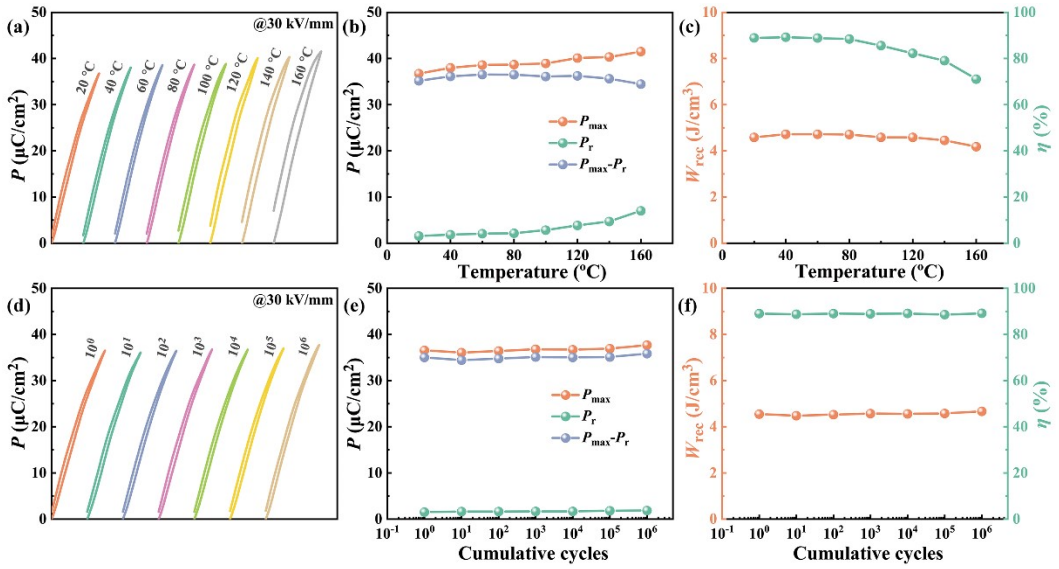


Fig. S13 Unipolar P - E curves of $x = 0.10$ at different (a) temperature, and (d) cumulative cycle numbers, and corresponding (b), (e) P_{\max} , P_r , $P_{\max}-P_r$, and (c), (f) W_{rec} and η .

Table S3 Comparison of E_b/E_{test} , W_{rec} and η between this work and recently reported BNT-, BTO-, KNN- and BFO-based relaxor ferroelectric ceramics.

Composition	E_b or E_{test} (kV/mm)	W_{rec} (J/cm^3)	η (%)	Ref.
0.62BLF-0.30BST-0.08KNN	69	16.3	85.9	This work
0.60BLF-0.30BST-0.10KNN	63	13.9	89.6	This work
BNT-based				
0.62Na _{0.5} Bi _{0.5} TiO ₃ -0.3Sr _{0.7} Bi _{0.2} TiO ₃ -0.08BiMg _{2/3} Nb _{1/3} O ₃	47	7.5	92	Energy Stor. Mater. 38 (2021) 113-120
0.8(0.95Bi _{0.5} Na _{0.5} TiO ₃ -0.05SrZrO ₃)-0.2NaNbO ₃	35	5.55	82.2	ACS Appl. Mater. Interfaces 13 (2021) 28484-28492
0.75Bi _{0.58} Na _{0.42} TiO ₃ -0.25SrTiO ₃	53.5	5.63	94	Energy Stor. Mater. 30 (2020) 392-400
0.8Bi _{0.5} Na _{0.5} TiO ₃ -0.2SrNb _{0.5} Al _{0.5} O ₃	52	6.64	96.5	Nano Energy 75 (2020) 105012
0.76(0.94Na _{0.5} Bi _{0.5} TiO ₃ -0.06BaTiO ₃)-0.24CaTi _{0.75} Ta _{0.2} O ₃	41	9.55	88	ACS Appl. Mater. Interfaces 14 (2022) 22263-22269
BT-based				

0.9(0.75BaTiO ₃ -0.25Na _{0.5} Bi _{0.5} TiO ₃)-0.1Bi(Zn _{0.2} Mg _{0.2} Al _{0.2} Sn _{0.2} Zr _{0.2})O ₃	27.3	3.74	82.2	Chem. Eng. J. 427 (2022) 131684
0.90BaTiO ₃ -0.10Bi(Mg _{0.5} Zr _{0.5})O ₃ @SiO ₂	34.5	3.41	85.1	Adv. Funct. Mater. 30 (2020) 2000191
0.6BaTiO ₃ -0.4Bi(Mg _{1/2} Ti _{1/2})O ₃	34	4.49	93	Nano Energy 67 (2020) 104264
0.9Ba _{0.65} Sr _{0.35} TiO ₃ -0.1Bi(Mg _{2/3} Nb _{1/3})O ₃	40	3.34	85.71	ACS Appl. Mater. Interfaces 12 (2020) 30289-30296
0.6(Ba _{0.75} Sr _{0.25})TiO ₃ -0.3Bi(Mg _{0.5} Hf _{0.5})O ₃	39	4.3	92	ACS Appl. Energy Mater. 3 (2020) 12254-12262
KNN-based				
0.85K _{0.5} Na _{0.5} NbO ₃ -0.15Bi(Ni _{0.5} Zr _{0.5})O ₃	87	8.09	88.46	Energy Stor. Mater. 45 (2022) 861-868
0.85K _{0.5} Na _{0.5} NbO ₃ -0.15Bi(Zn _{2/3} Ta _{1/3})O ₃	60	6.7	92	Adv. Funct. Mater. (2021) 2111776
0.975K _{0.5} Na _{0.5} NbO ₃ -0.025LaBiO ₃	34	3.60	74.2	ACS Appl. Mater. Interfaces 13 (2021) 28472-28483
0.925(K _{0.5} Na _{0.5})NbO ₃ -0.075Bi(Zn _{2/3} (Ta _{0.5} Nb _{0.5}) _{1/3})O ₃	30.7	4.02	87.4	J. Materomics 7 (2021) 780-789
0.9K _{0.5} Na _{0.5} NbO ₃ -0.1BiFeO ₃	20.6	2	61	Nano Energy 58 (2019) 768-777
BF-based				
0.35BiFeO ₃ -0.65SrTiO ₃	75	8.4	90	Small 18 (2022) 2106515
0.85(0.65BiFeO ₃ -0.35BaTiO ₃)-0.15Sr _{0.7} Bi _{0.2} TiO ₃	33	4.95	73	Chem. Eng. J. 412 (2021) 127555
0.88(0.67BiFeO ₃ -0.33BaTiO ₃)-0.12Na _{0.73} Bi _{0.09} NbO ₃	41	5.57	83.8	Chem. Eng. J. 417 (2021) 127945
0.57BiFeO ₃ -0.33BaTiO ₃ -0.1NaNbO ₃	36	8.12	90	Adv. Energy Mater. 10 (2020) 1903338
0.54BiFeO ₃ -0.4SrTiO ₃ -0.06BiMg _{2/3} Nb _{1/3} O ₃ -0.03Nb ₂ O ₅	46	8.2	74.1	Energy Environ. Sci. 13 (2020) 2938-2948
Bi _{0.83} Sm _{0.17} Fe _{0.95} Sc _{0.05} O ₃	23	2.21	76	J. Eur. Ceram. Soc. 39 (2019) 2331-2338
0.61BiFeO ₃ -0.33(Ba _{0.8} Sr _{0.2})TiO ₃ -0.06La(Mg _{2/3} Nb _{1/3})O ₃ +0.1wt.% MnO ₂ +2wt.% BaCu(B ₂ O ₅)	23	3.38	59	J. Eur. Ceram. Soc. 39 (2019) 2673-2679
0.43BiFeO ₃ -0.45SrTiO ₃ -0.12BaTiO ₃ +0.1wt.%MnO ₂	49	7.3	86.3	J. Am. Ceram. Soc. Doi: 10.1111/jace.18589